International Journal of Engineering and Information Systems (IJEAIS)
ISSN: 2643-640X
Vol. 6 Issue 10, October - 2022, Pages: 32-40

Recording of Industrial Robot Pedestal Vibration Using Programmable ADXL335 Accelerometer for Safety Assurance

Panagiotis Rizos [1], Anastasia Kotsiaridi [2], Penelope Marmaridou [3]

1 Department of Informatics, School of Information Sciences and Technology, Athens University of Economics and Business, Athens, Greece.
2 Department of Mechanical Engineering, School of Engineering, University of Thessaly, Volos, Greece.
3 Department of Environmental Engineering, Democritus University of Thrace, Xanthi, Greece.

Abstract— *Industrial robotic arms during their movement from point-to-point show vibrations that can affect the grip of an object or be destructive to the pedestal base. The scenario of the destruction of the pedestal would result in the robotic arm permanently stopping its operation for safety reasons until it is repaired. Collecting and analyzing necessary data can anticipate and prevent such negative or unwanted situations. This paper presents measurements taken during operation on a six-axis and 3,124mm reach robotic arm using the ADXL335 three-axis accelerometer sensor. The programmable microcontroller Arduino Mega 2560 was used to connect the accelerometer and record the data to the computer. The experimental results showed very small rates of dynamic acceleration resulting from vibration during the momentary speed increases of the robotic arm in five different cycles and have no future consequences for robot pedestal and facility safety.*

Keywords— robot, acceleration, vibration

1. INTRODUCTION

From a static point of view, the low stiffness of industrial robots during robotic work requires the production of defined products. From a dynamic point of view, when low-stiffness robots are used, low-frequency vibrations can be induced, resulting in a decrease in the quality of the produced product. The generated vibrations cause a reduction in the life of the end effector of the gripper, can damage the joints of the robot, and even cause damage to the pedestal [1]. Sometimes, combinations of serial and parallel kinetic chains have been suggested to increase robot stiffness.

The pedestal of industrial robots is an important factor for its smooth and safe operation during the execution of cycles. The direct support of the arm on the industrial floor is clearly one of the best solutions. However, if the entire robotic process to be performed needs a relative height in relation to the robot base, then it is necessary to create an additional support base of corresponding height [2]. The additional pedestal is bolted below the main robot body base to add height and thus more reach to the finished tool. The vibrations caused during the operation of the robot can momentarily or in the future, in addition to affecting the main body of the robot such as the joints and the final tool, affect the pedestal. High vibration values that are continuous in a robot moving at 100% of its speed for 24 hours, 7 days per week could cause the additional support to crack, loosen its screws, and even detach the main body of the robot above it [3].

In this paper we present the results of the vibration measurements made on the pedestal of six-axis and 3,124mm reach robotic arm. The data were collected with the help of the ADXL335 accelerometer sensor mounted on the add-on mount and recorded for analysis on the computer through the Arduino Mega 2560 programmable microcontroller [4]. Then we present how we can collect and analyze such data. Below is the Arduino Mega 2560 programmable microcontroller board and the sensor chosen to collect the data. Finally, we present the measurements were taken for 5 different movements of the robot in five corresponding different cycles.

2. MATERIALS AND METHODS

2.1 Arduino Mega 2560 and ADXL 335 Accelerometer

To implement the measurement that will detect the existence of vibrations, we used the Arduino Mega 2560 board. The sensor will be connected to this board. It is an open-source microcontroller suitable for embedded systems development, which has inputs and outputs, and is programmed in a variant of the C++ language called Wiring.

The ATmega2560 microprocessor is mounted on the Arduino Mega 2560 microcontroller and 54 digital and analog I/O pins are mounted in the circumference. Of these pins, 15 are PWM Outputs, 16 pins are analog Inputs, and 4 pins are serial communication ports. In these pins, the connection is made to various electronic elements and sensors that we have chosen, such as LEDs, accelerometers, motors, etc. The Arduino Mega 2560 that was utilized, apart from the aforementioned features, also has a 16 MHz crystal oscillator and the ability to connect to AC-DC power supply for its operation [5].

Arduino programming is done by connecting it to our computer through a USB port that it has. An important feature of the microcontroller is the visualization of the data during the operation of the sensors we have connected, since of course their programming has preceded [6].

The sensor that we used ADXL335 is a small, thin, low power, complete 3-axis accelerometer with signal conditioned voltage outputs. Measures acceleration with a minimum full-scale range of ±3 g. It can measure the static acceleration of gravity in tilt-sensing applications, as well as dynamic acceleration resulting from motion, shock, or vibration. The bandwidth of the accelerometer was selected using the CX, CY, and CZ capacitors at the XOUT, YOUT, and ZOUT pins. Bandwidths can be selected to suit the application, with a range of 0.5 Hz to 1600 Hz for the X and Y axes, and a range of 0.5 Hz to 550 Hz for the Z axis [7].

The sensor is a polysilicon surface-micromachined structure built on top of a silicon wafer. Polysilicon springs suspend the structure over the surface of the wafer and provide a resistance against acceleration forces. Deflection of the structure is measured using a differential capacitor that consists of independent fixed plates and plates attached to the moving mass [8].

2.2 Measurement Architecture and ADXL335 Code

The measurements were made while the robot was operating without payload at the end effector. The robot features are six-axis and 3,124mm reach. Six-axis robots are a type of articulated robot and the most common for industrial manufacturing. The pedestal is square shaped, consists of solid iron 20 mm thick, 800mm height and is bolted to the ground of the facility. The robot was running at 100% of its speed making linear movements at 1600mm/s. The sensor was glued to the pedestal of the robot with the +X pointing in the same direction as the +X of the robot's coordinates [9]. The sensor was connected to the microcontroller and it in turn to the computer. The connection diagram is shown in “Fig. 1”. The microcontroller was programmed to see the ADXL 335 sensor with the code shown in Table 1.

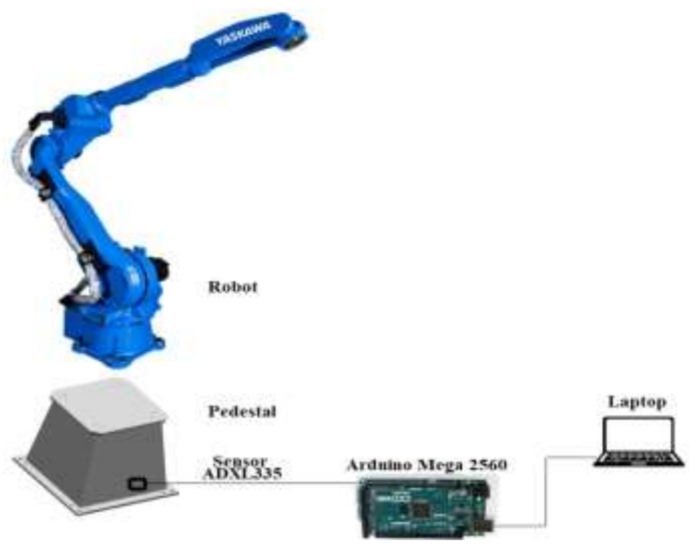

Fig. 1. *Measurement architecture on a six-axis robot.*

Few of sensor specs are dependent on the power delivered to the chip. The sensitivity (mV/g) is stated to be ratiometric, and the example given is that when delivering 3V to the power supply, the sensitivity is 300 mV/g[10]. Another ratiometric value is the “0g bias”. The accelerometer chip can detect negative acceleration, but it doesn’t output a negative voltage signal. The middle point of the power supply voltage range should be considered the 0 point. Power supply voltage is 3.3V, so we must consider 1.6V as the zero point. If the accelerometer is turned upside-down, it shall undergo -1g of force. The voltage output would be 1.27V.

Table 1. Arduino Mega2560 code for ADXL335 sensor

```
int xAxisPin = A0;
int yAxisPin = A1;
int zAxisPin = A2;
int xAxisValADC = 0;
int yAxisValADC = 0;
int zAxisValADC = 0;
float xAxisValmV = 0;
```

```
float yAxisValmV = 0;
float zAxisValmV = 0;
int ADCMaxVal = 1023;
float mVMaxVal = 5000;
float supplyMidPointmV = 3230 / 2;
int mVperg = 323;
float mVPerADC = mVMaxVal / ADCMaxVal;
void setup() {
Serial.begin(9600);
pinMode(A0, INPUT);
pinMode(A1, INPUT);
pinMode(A2, INPUT);   }
void loop() {
xAxisValADC = analogRead(xAxisPin);
yAxisValADC = analogRead(yAxisPin);
zAxisValADC = analogRead(zAxisPin);
xAxisValmV = xAxisValADC * mVPerADC;
yAxisValmV = yAxisValADC * mVPerADC;
zAxisValmV = zAxisValADC * mVPerADC;
Serial.print((xAxisValmV - supplyMidPointmV) / mVperg);
Serial.print("\t");
Serial.print((yAxisValmV - supplyMidPointmV) / mVperg);
Serial.print("\t");
Serial.print((zAxisValmV - supplyMidPointmV) / mVperg);
Serial.print("\t");
Serial.println();
delay(100); }
```

2.3 ADXL335 Accelerometer Data

Five vibration measurements were taken at the pedestal of the robot. Each measurement involved a separate movement of the robot from one cycle. Specifically in the first cycle of the robot, the vibrations were measured when the robot remained stationary in its safe position. In the second cycle of the robot operation, the vibrations were measured when the robot moved in a linear manner forward to +X. In the third cycle of the robot, the vibrations were measured when the robot moved in a linear direction to the left at +Y. In the fourth cycle of the robot, the vibrations were measured when the robot moved in a linear direction to the right to -Y. In the fifth cycle of the robot, the vibrations were measured when the robot moved in a linear manner to -X from the starting position. The measurements taken in the five cycles of the robot are presented below.

In joint motion the path is predictable, faster and is used for picking and placing parts when the path does not need to be precise [11]. On the other hand, in linear motion the path is important and is used when the motion must be continuously controlled to follow a path with accuracy. Linear motion takes more time and is used for applications such as cutting or painting [12].

In the first cycle the robot remains immovable in its starting position. The ADXL335 sensor is composed of a proof mass (containing 4 parts M1, M2, M3 and M4) which is kept in a continuously oscillating movement so that it reacts to the coriolis effect. They move inward and outward simultaneously in the horizontal plane [13]. When the structure starts rotating, the Coriolis force acting on the moving proof mass changes the direction of the vibration from horizontal to vertical.

In “Fig. 2” we see that the Z axis remains constant. The X axis values are 1.11g that is equal to 10.885 m/s^2. We know that 1g is equal to 9.806 m/s^2. When an angular rate is applied along the Z-axis, M2 and M4 will move in the same horizontal plane in opposite directions. This causes the yaw angle to change hence it is called Yaw Mode. Also, the X and Y axes do not change values. The X and Y axes values are 0.11g that is equal to 1.078 m/s^2. This makes sense because the robot is in an initial position and does not make any movement. The values on X and Y axes are very low due to the vibrations of the ground [14].

Vibration Data 1

TIME	X	Y	Z
13:27:59.99	0.11	0.11	1.11
13:28:00.09	0.11	0.11	1.11
13:28:00.19	0.11	0.11	1.11
13:28:00.29	0.11	0.11	1.11
13:28:00.39	0.11	0.11	1.11
13:28:00.50	0.11	0.11	1.11
13:28:00.60	0.11	0.11	1.11
13:28:00.70	0.11	0.11	1.11
13:28:00.80	0.11	0.11	1.11
13:28:00.90	0.11	0.11	1.11
13:28:01.00	0.11	0.1	1.11
13:28:01.11	0.11	0.11	1.11
13:28:01.20	0.11	0.11	1.11
13:28:01.31	0.11	0.11	1.11
13:28:01.41	0.11	0.11	1.11

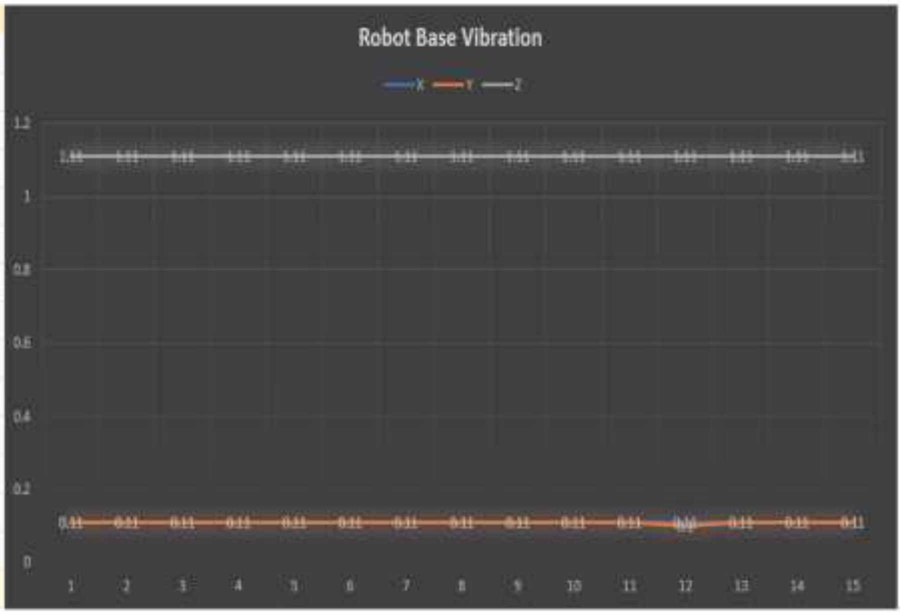

Fig. 2. *Vibration data of the first robot cycle.*

In the second cycle, the vibrations were measured when the robot moved linear forward to +X. In "Fig. 3" it is evident that the Z axis remains constant. The Y axis has increased to 0.13 g that is equal to 1.274 m/s^2. The X axis has increased to 0.25g that is equal to 2.451 m/s^2. This difference is relatively large and is not recorded during the entire movement. This is natural because the robot performs the linear motion MOVL forward to +X. The acceleration increases and an amount of vibration appears on the robot pedestal. Nevertheless, we see that even in this movement of robot the vibration values are not large.

Vibration Data 2

TIME	X	Y	Z
13:28:43.36	0.11	0.11	1.11
13:28:43.46	0.11	0.11	1.11
13:28:43.56	0.13	0.11	1.11
13:28:43.66	0.13	0.1	1.11
13:28:43.76	0.08	0.13	1.11
13:28:43.86	0.1	0.13	1.11
13:28:43.97	0.25	0.04	1.11
13:28:44.07	0.13	0.11	1.11
13:28:44.17	0.11	0.11	1.11
13:28:44.27	0.11	0.11	1.11
13:28:44.37	0.13	0.11	1.11
13:28:44.47	0.13	0.11	1.11
13:28:44.58	0.11	0.11	1.11
13:28:44.68	0.13	0.11	1.11
13:28:44.78	0.11	0.11	1.11

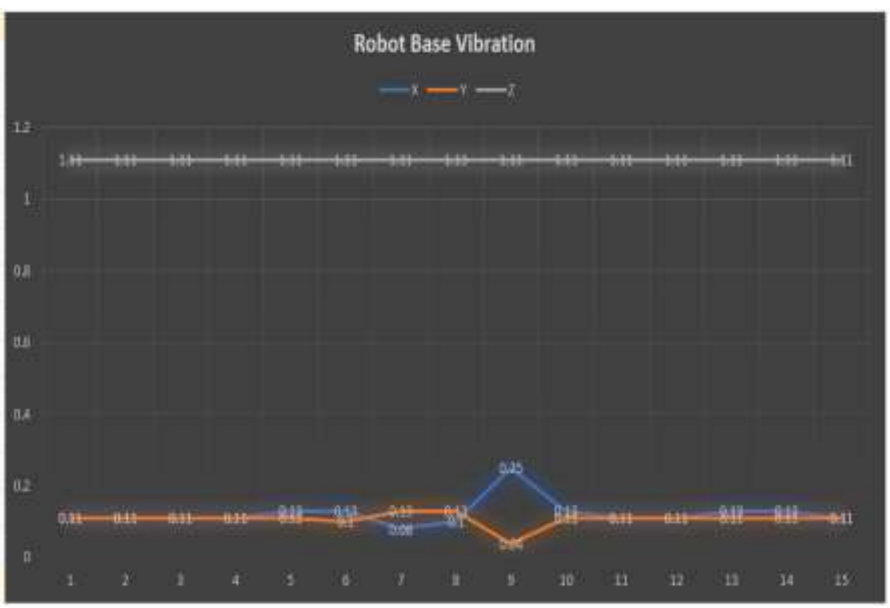

Fig. 3. *Vibration data of the second robot cycle.*

International Journal of Engineering and Information Systems (IJEAIS)
ISSN: 2643-640X
Vol. 6 Issue 10, October - 2022, Pages: 32-40

In the third cycle of the robot, the vibrations were measured when the robot moved linear to the left at +Y. In “Fig. 4” we see that the Z axis remains constant with the values of 1.11g. The Y axis has increased to 0.13 g that is equal to 1.274 m/s^2. The X axis has increased to 0.14g that is equal to 1.372 m/s^2 . This difference is small and is not recorded during the entire movement. At this moment the robot performs the linear motion MOVL to +Y and the vibration values are not large.

At this point, in the third cycle the robot has made a relative extension of its links. The end point of the robot is located 3 meters from the center of the base. When the robot moves close to its center and not far from it, then the movements are faster and with more precision. In the specific case of the measurements, operations were not characterized by accuracy per repetition [15].

Acceleration creates vibrations at each joint of the robot. This has as much to do with the distance from the center of the robot's pedestal as it does with whether there is an object at the robot's endpoint. The weight of the object will slightly reduce the speed of the robot and increase the vibration values that would be present in the joints and thus the pedestal of the robot [16].

In our experiments we only deal with vibrations at the pedestal of the robot. It is worth noting that the value displayed on the Z axis 1.26g that is equal to 12.356 m/s^2 is increased but then falls to 1.11g. The attenuation of the vibrational waves is very rapid going down from 1.26g to 1.13g, 1.1g and finally to 1.11g where it remains constant.

Vibration Data 3

TIME	X	Y	Z
13:29:15.66	0.11	0.11	1.11
13:29:15.76	0.11	0.1	1.11
13:29:15.86	0.13	0.07	1.26
13:29:15.96	0.14	0.1	1.13
13:29:16.06	0.11	0.13	1.1
13:29:16.17	0.1	0.11	1.11
13:29:16.27	0.1	0.11	1.11
13:29:16.37	0.11	0.11	1.11
13:29:16.47	0.11	0.11	1.11
13:29:16.57	0.1	0.11	1.11
13:29:16.67	0.1	0.1	1.11
13:29:16.77	0.1	0.1	1.11
13:29:16.87	0.1	0.1	1.11
13:29:16.98	0.1	0.1	1.11
13:29:17.08	0.1	0.11	1.11

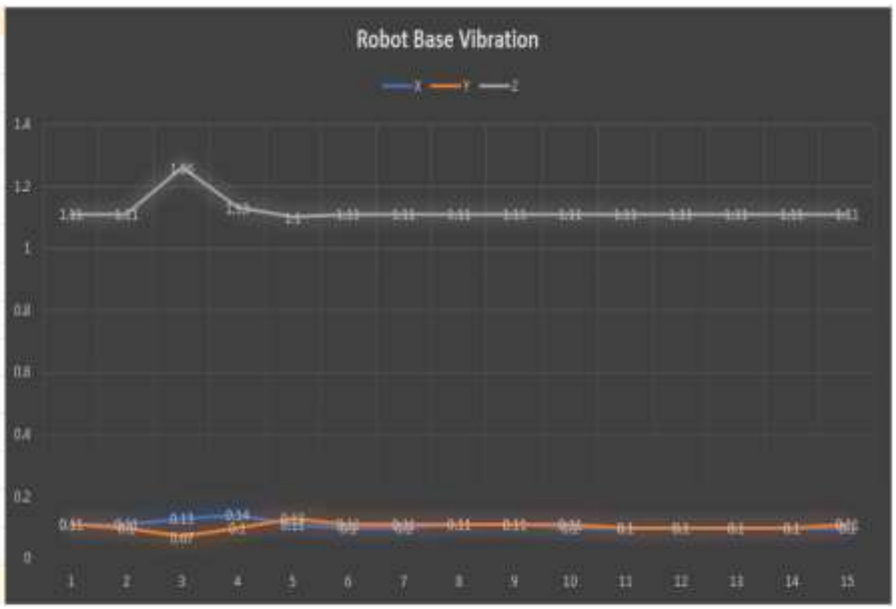

Fig. 4. *Vibration data of the third robot cycle.*

International Journal of Engineering and Information Systems (IJEAIS)
ISSN: 2643-640X
Vol. 6 Issue 10, October - 2022, Pages: 32-40

In the fourth cycle of the robot, the vibrations were measured when the robot moved linear right to -Y. In “Fig. 5” we see that the Z axis remains constant. The Y axis has increased to 0.13 g that is equal to 1.274 m/s^2. The X axis has increased also to 0.13g that is equal to 1.274 m/s^2. The robot performs the linear motion MOVL to -Y. In this movement of robot, the vibration values are not large. The values 0.1g, 0.11g and 0.13g appear and disappear. This happens due to the propagation of vibration waves that end up at the pedestal of the robot. The pedestal consists of solid iron 20 mm thick and is bolted to the ground of the facility. From this we conclude that the thickness of the pedestal and its material plays an important role in the rapid attenuation of the vibration waves coming from the sudden accelerations of the robot [17]. In the particular case of experiments there is no cause for concern because the vibration values are very low even the decay time of the vibration waves is low.

Vibration Data 4

TIME	X	Y	Z
13:29:48.26	0.13	0.1	1.11
13:29:48.36	0.13	0.1	1.11
13:29:48.46	0.11	0.11	1.11
13:29:48.56	0.11	0.11	1.11
13:29:48.67	0.1	0.11	1.11
13:29:48.77	0.1	0.11	1.11
13:29:48.87	0.11	0.11	1.11
13:29:48.97	0.13	0.1	1.11
13:29:49.07	0.1	0.11	1.11
13:29:49.17	0.1	0.11	1.11
13:29:49.28	0.1	0.13	1.11
13:29:49.38	0.11	0.11	1.11
13:29:49.48	0.1	0.1	1.11
13:29:49.58	0.13	0.1	1.11
13:29:49.68	0.11	0.1	1.11

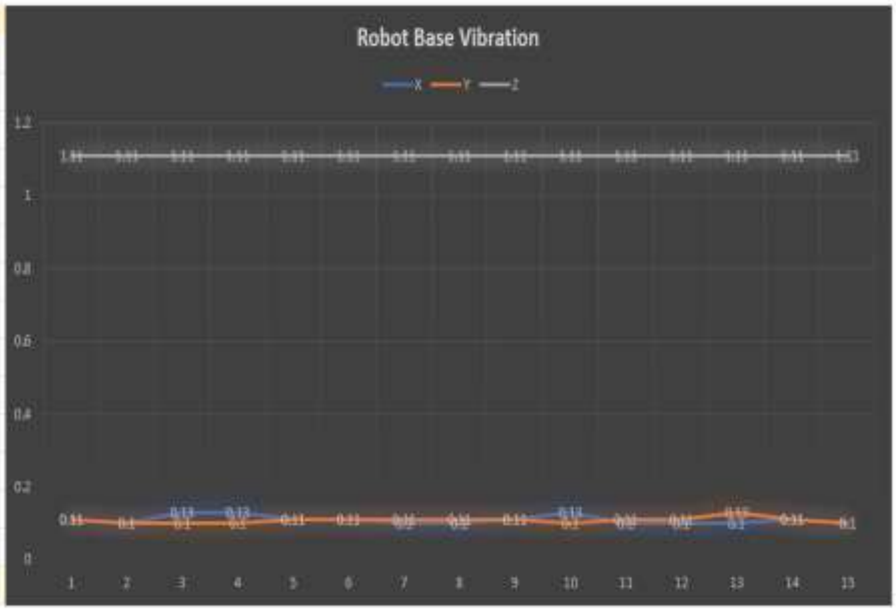

Fig. 5. *Vibration data of the fourth robot cycle.*

In the fifth cycle of the robot, the vibrations were measured when the robot moved linear to -X to the starting position. In “Fig. 6” it can be observed that the Z axis increased to 1.13g that is equal to 11.081 m/s^2. The Y axis has increased to 0.14 g that is equal to 1.372 m/s^2. The X axis has increased to 0.14g that is equal to 1.372 m/s^2. The robot performs the linear motion MOVL to -X behind the starting position. In this robot movement, the vibration values are not large.

International Journal of Engineering and Information Systems (IJEAIS)
ISSN: 2643-640X
Vol. 6 Issue 10, October - 2022, Pages: 32-40

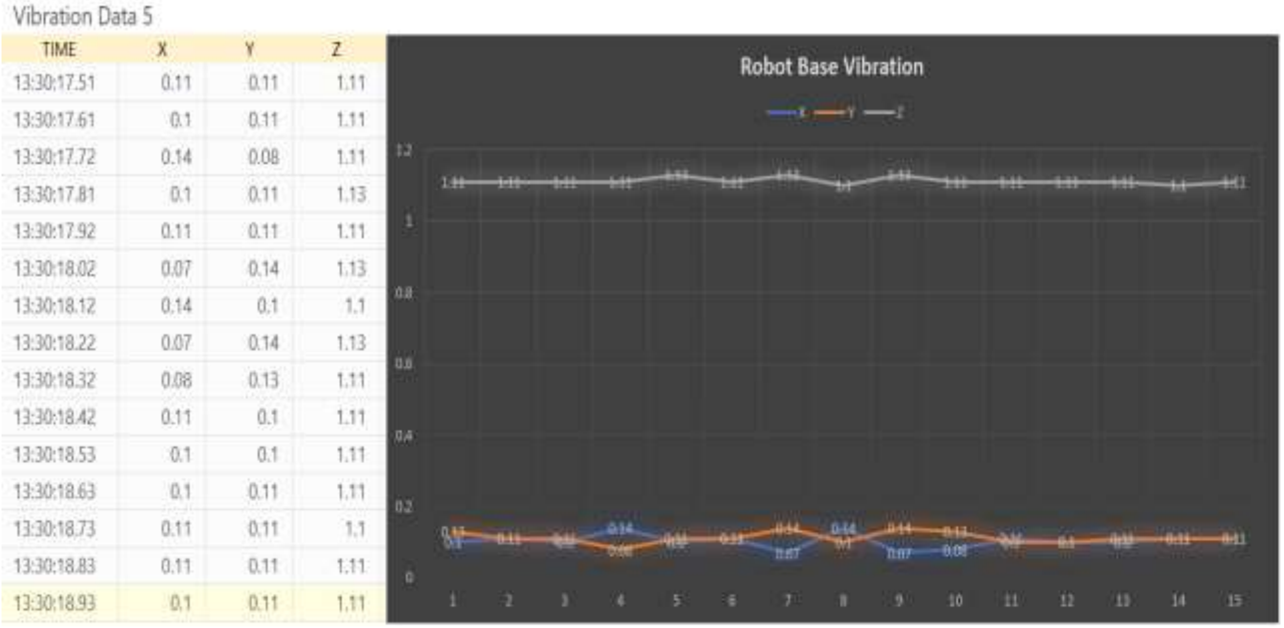
Vibration Data 5

TIME	X	Y	Z
13:30:17.51	0.11	0.11	1.11
13:30:17.61	0.1	0.11	1.11
13:30:17.72	0.14	0.08	1.11
13:30:17.81	0.1	0.11	1.13
13:30:17.92	0.11	0.11	1.11
13:30:18.02	0.07	0.14	1.13
13:30:18.12	0.14	0.1	1.1
13:30:18.22	0.07	0.14	1.13
13:30:18.32	0.08	0.13	1.11
13:30:18.42	0.11	0.1	1.11
13:30:18.53	0.1	0.1	1.11
13:30:18.63	0.1	0.11	1.11
13:30:18.73	0.11	0.11	1.1
13:30:18.83	0.11	0.11	1.11
13:30:18.93	0.1	0.11	1.11

Fig. 6. *Vibration data of the fifth robot cycle.*

3. ROBOT SAFETY AND ACCELEROMETER DATA

The stability of the robot's pedestal plays a big role in the smooth operation of the robot itself as well as the installation that surrounds it (safety fence in “Fig. 7”) and possibly the workers outside it who perform various tasks. Very high values that would cause micro-cracks in the robot's mounting pedestal and would be destructive over time and if the robot continued to move at high speeds and accelerations [18].

From the measured results we observe very small vibration values during the accelerations of the robot which are not alarming and do not affect the support pedestal. Vibration values during robot accelerations decrease rapidly and remain stable. The robot can operate normally without any problem performing the production cycles. Also, workers outside the robotic facility can continue to work with a sense of security [19].

The safety of the robotic installation and the workers moving outside the robot cage plays an important role in the smooth continuation of productivity [20]. The company or industry itself that has installed a robotic arm can ensure the safety of its own workers and protect the investment of a robotic installation.

In terms of occupational health and safety, vibrations occurring from sound may pose a major threat to the robot's construction integrity. If not properly secluded from the rest of the machinery inside industrial spaces, or from the personel passing by during working hours, there is a high probability of accident and serious injury [21].

More specifically, high sound levels in industrial environments result in damage of structural elements, such as walls, and immovable equipment, like machinery. The phenomenon which causes the cracking of those elements due to sound is called “synchronization”. The natural frequency of the building materials and the equipment equals the frequency of the sound, leading to structural elements falling apart and collapsing. Moreover, the sounds made from the robot itself threaten the integrity of the installation. Sound waves alter the atmospheric pressure around the pedestal of the robot. The pressure fluctuations push and pull the materials, diminishing their technical traits and accelerating the damage process [22].

As a consequence, the installation is collapsing after a short period of time. As it falls down, it may injure people who are working nearby or passing by. If other kinds of equipment are installed and operating in a short distance, there is high probability of bearing damage from the collision of the mechanical parts, causing a “butterfly effect” that will cease production processes [23].

To avoid such incidents, several actions can be taken. First and foremost, sound-absorbing materials can be used to construct a protective frame, therefore reducing the negative impact. However, this can be considered a non-viable option in terms of finance and expenditure, taking into consideration the economic background of each industry. Second, there must be set boundaries to specify the range of the robotic arm(s) movements. This can be achieved by coloring the floor area around the robot and installing the proper safety warning signs [24].

Fig. 7. *A six-axis robot in a safety fence (Source: www.mmci-automation.com/palletizing-safety).*

4. CONCLUSION

In this paper we have presented the vibration measurements from the robot pedestal. The measurements were taken for 5 different movements of the robot in five corresponding different cycles. For these measurements we used the ADXL335 sensor and programmed it through the microcontroller Arduino Mega2560 so that we could record and analyze the data on our computer. The measurements showed that there are very small percentages of vibrations during accelerations that diminish very quickly and stabilize. Other small vibration values are recorded even when the robot is at the starting position and are due to ground vibrations and the technical characteristics of the sensor. All the measurements in 5 movements are not alarming and cannot cause problems in the robot pedestal in the future, the robot can continue to work at 100% of its speed and workers outside the robotic facility can continue to work with a sense of safety.

5. REFERENCES

[1] Kraus, Karel, et al. "Mechatronic robot arm with active vibration absorbers." Journal of Vibration and Control 26.13-14 (2020): 1145-1156.

[2] Rui-li, Chang, et al. "Workspace Analysis of CNC Load-Unload Material Robot." 2019 2nd World Conference on Mechanical Engineering and Intelligent Manufacturing (WCMEIM). IEEE, 2019.

[3] Zheng, Kunming. "Research on intelligent vibration suppression control of high-speed lightweight Delta robot." Journal of Vibration and Control (2021): 10775463211024888.

[4] Jatakar, Keshav H., et al. "Vibration monitoring system based on ADXL335 accelerometer and Arduino Mega2560 interface." JOURNAL OF ALGEBRAIC STATISTICS 13.2 (2022): 2291-2301.

[5] Myasischev, Olexander, et al. "Creation of a Rotor-Type UAV with Flight Controllers, Based On a ATmega2560 and STM32f405 Microprocessors." (2020).

[6] Suciyati, Sri Wahyu, and GURUM A. PAUZI GURUM A PAUZI. "An analysis of data acquisition system of temperature, oxygen, and carbon dioxide in refrigerator with arduino mega 2560." Jurnal ilmiah pendidikan fisika Al-Biruni 10.1 (2021): 119-127.

[7] Jatakar, Keshav H., et al. "Vibration monitoring system based on ADXL335 accelerometer and Arduino Mega2560 interface." JOURNAL OF ALGEBRAIC STATISTICS 13.2 (2022): 2291-2301.

[8] Malik, Haroon, and Anam Mazhar. "EyeCom-An Innovative Approach for Computer Interaction." Procedia Computer Science 151 (2019): 559-566.

[9] Shadrin, Gennady K., et al. "Application of compensation algorithms to control the movement of a robot manipulator." Acta Polytechnica Hungarica 17.1 (2020): 191-214.

[10] Gopalakrishna, Gururaj K., and Srinivasa Pai Padubidre. "Development of low cost system for condition monitoring of rolling element bearing using MEMS based accelerometer." AIP Conference Proceedings. Vol. 2080. No. 1. AIP Publishing LLC, 2019.

[11] Wada, Kentaro, Kei Okada, and Masayuki Inaba. "Joint learning of instance and semantic segmentation for robotic pick-and-place with heavy occlusions in clutter." 2019 International Conference on Robotics and Automation (ICRA). IEEE, 2019.

[12] Carossa, Massimo, et al. "Individual mandibular movement registration and reproduction using an optoeletronic jaw movement analyzer and a dedicated robot: a dental technique." BMC Oral Health 20.1 (2020): 1-8.

[13] Ayazi, Farrokh, et al. "High-q timing and inertial measurement unit chip (TIMU) with 3D wafer-level packaging." 2019 IEEE Custom Integrated Circuits Conference (CICC). IEEE, 2019.

[14] Ismail, Mohd Ismifaizul Mohd, et al. "A review of vibration detection methods using accelerometer sensors for water pipeline leakage." IEEE access 7 (2019): 51965-51981.

[15] Wu, Jinhui, et al. "A moment approach to positioning accuracy reliability analysis for industrial robots." IEEE Transactions on Reliability 69.2 (2019): 699-714.

[16] Shan, Xiaobiao, et al. "Linear system identification and vibration control of end-effector for industrial robots." Applied Sciences 10.23 (2020): 8537.

[17] Zhizhin, G. N., et al. "Surface electromagnetic wave propagation on metal surfaces." Surface Polaritons. Amsterdam: North-Holland, 1982. 93-144.

[18] Song, Siyang, et al. "Modeling and control of inherently safe robots with variable stiffness links." Robotics and Autonomous Systems 120 (2019): 103247.

[19] Gihleb, Rania, et al. "Industrial robots, workers' safety, and health." Labour Economics 78 (2022): 102205.

[20] Choi, HeeSun, and Naomi Swanson. "Understanding worker trust in industrial robots for improving workplace safety." Trust in Human-Robot Interaction. Academic Press, 2021. 123-141.

[21] Adel Badri, Bryan Boudreau-Trudel, Ahmed Saâdeddine Souissi, Occupational health and safety in the industry 4.0 era: A cause for major concern Safety Science, Volume 109, 2018, Pages 403-411, ISSN 0925-7535, https://doi.org/10.1016/j.ssci.2018.06.012.

[22] Evgeniy Bryndin. Increase of Safety Use Robots in Industry 4.0 by Developing Sensitivity and Professional Behavioral Skills. American Journal of Mechanical and Industrial Engineering. Vol. 5, No. 1, 2020, pp. 6-14. doi: 10.11648/j.ajmie.20200501.12

[23] M. Erol , "OCCUPATIONAL HEALTH AND WORK SAFETY SYSTEMS IN COMPLIANCE WITH INDUSTRY 4.0: RESEARCH DIRECTIONS", International Journal of eBusiness and eGovernment Studies, vol. 11, no. 2, pp. 119-133, Dec. 2019, doi:10.34111/ijebeg.20191123

[24] Savela, N., Turja, T. & Oksanen, A. Social Acceptance of Robots in Different Occupational Fields: A Systematic Literature Review. Int J of Soc Robotics 10, 493–502 (2018). https://doi.org/10.1007/s12369-017-0452-5